The Analysis of Nonlinear Synaptic Transmission

HOWARD I. KRAUSZ and W. OTTO FRIESEN

From the Department of Neurosciences, University of California, San Diego, La Jolla, California 92093, and the Department of Physiology and Biophysics, University of Texas Medical Branch, Galveston, Texas 77550. Dr. Krausz's present address is the Department of Physiology and Biophysics, University of Texas Medical Branch, Galveston, Texas 77550, and Dr. Friesen's is the Department of Biology, University of Virginia, Charlottesville, Virginia 22903.

ABSTRACT In order to characterize synaptic transmission at a unitary facilitating synapse in the lobster cardiac ganglion, a new nonlinear systems analysis technique for discrete-input systems was developed and applied. From the output of the postsynaptic cell in response to randomly occurring presynaptic nerve impulses, a set of kernels, analogous to Wiener kernels, was computed. The kernels up to third order served to characterize, with reasonable accuracy, the input-output properties of the synapse. A mathematical model of the synapse was also tested with a random impulse train and model predictions were compared with experimental synaptic output. Although the model proved to be even more accurate overall than the kernel characterization, there were slight but consistent errors in the model's performance. These were also reflected as differences between model and experimental kernels. It is concluded that a random train analysis provides a comprehensive and objective comparison between model and experiment and automatically provides an arbitrarily accurate characterization of a system's input-output behavior, even in complicated cases where other approaches are impractical.

INTRODUCTION

At a variety of well-known synapses and neuromuscular junctions the amplitude of each impulse-evoked PSP or EPP depends on the preceding pattern of impulse activity (Bullock, 1943; Del Castillo and Katz, 1954; Dudel and Kuffler, 1961; Hagiwara and Bullock, 1957; Mallart and Martin, 1967; Takeuchi and Takeuchi, 1962). Increases in PSP amplitude are generally described as facilitation or potentiation, while decreases are referred to as defacilitation, antifacilitation, or depression. Since a single PSP is in effect the impulse response of a synapse, transmission is by definition nonlinear at synapses where PSP amplitudes vary.

Nonlinear synaptic transmission is one of the primary methods by which neural signals are modified and has been hypothesized to account for such behavioral phenomena as conditioning and habituation (Carew and Kandel, 1974; Castellucci et al., 1976). In order to assess accurately the information transformation at a particular synapse, a quantitative understanding of any nonlinearities in transmission is of fundamental importance.

In the study reported here, a new technique for analyzing nonlinear synaptic transmission was applied to a unitary facilitating synapse in the lobster cardiac ganglion. From the results of random stimulation of the synapse with a Poisson train of presynaptic impulses, a reasonably accurate characterization of the nonlinear input-output properties of the synapse is developed. This "white-noise" characterization of the nonlinear synaptic transfer function is then compared with the predictions of a model of the synapse (Friesen, 1975). This test application of the Poisson impulse train analysis method was motivated largely by the questions listed below and answered as well as possible in the Discussion.

(*a*) Will the Poisson train analysis yield an accurate characterization of the nonlinear synaptic transfer properties?

(*b*) Does the model of the synapse, which was constructed from the results of many conditioning volley-test stimulus type experiments accurately account for the results of Poisson stimulation of the living synapse? How does the accuracy of the model compare with that of the Poisson train analysis? (See *a* above.)

(*c*) Which of the two approaches, "white-noise" or "by guess and by golly" modeling, yields the synaptic transfer properties in the simplest and most efficient manner? What are their respective advantages and disadvantages?

(*d*) Could the Friesen model of the synapse have been constructed from the results of Poisson train experiments?

(*e*) Does the Poisson train analysis lead to any new insights about the synapse? For example, can the model of the synapse be simplified? What new experiments are suggested?

MATERIALS AND METHODS

Theory of Nonlinear System Characterization through Poisson Stimulation

The Poisson train analysis method applies to systems whose output $y(t)$ can be represented by a Volterra series (1) (Volterra, 1959) involving the input $x(t)$ and a set of kernels $k_i(\tau_1, \ldots, \tau_i)$.

$$y(t) = k_0 + \int_{-\infty}^{\infty} k_1(\tau)x(t-\tau)d\tau + \int_{-\infty}^{\infty}\int_{-\infty}^{\infty} k_2(\tau_1, \tau_2)x(t-\tau_1)x(t-\tau_2)d\tau_1 d\tau_2 + \ldots . \quad (1)$$

A large class of continuous time-invariant nonlinear systems with finite memory may be approximated by a Volterra series.

Wiener (1958) showed that the Volterra series (1) can be rewritten as a series of orthogonal functionals (Wiener series) provided the input $x(t)$ is a Gaussian white-noise signal. Lee and Schetzen (1965) suggested that the Wiener kernels, which characterize a particular nonlinear system, be computed from input-output cross correlations given a white-noise input. Recently, the Wiener technique as modified by Lee and Schetzen has been applied to a number of nonlinear biological systems (e.g., Bryant and Segundo, 1976; Lipson, 1975; Marmarelis and Naka, 1973*a*,*b*,*c*; McCann, 1974; Moore et al., 1975; Stark, 1968).

Since the input to the lobster cardiac ganglion synapse is a sequence of discrete presynaptic nerve impulses, each of which may be regarded as a Dirac delta function (Gerstein and Kiang, 1960), the system cannot be tested with continuous Gaussian white-noise and the Wiener method is not applicable. However, analogous to the Wiener series, a new orthogonal series for such point process systems can be derived from (1) given a Poisson impulse train input.

The simplest way to create such a series is to write a Volterra series, with kernels different from those in (1), where integrations along the kernel diagonals (cases where two or more of the τ's are equal) are now excluded as denoted below (Brillinger, 1975; Krausz, 1975; Krausz and Friesen, 1975)

$$y(t) = G_0[h_0, x(t)] + G_1(h_1, x(t)] + \ldots, \tag{2}$$

where

$$G_0 = h_0$$

$$G_1 = \int_{-\infty}^{\infty} h_1(\tau)x(t - \tau)d\tau$$

$$G_2 = \int_{-\infty}^{\infty}\int_{-\infty}^{\infty} h_2(\tau_1, \tau_2)x(t - \tau_1)x(t - \tau_2)d\tau_1 d\tau_2$$

$$\tau_1 \neq \tau_2.$$

When the input to this restricted diagonal Volterra series (2) is the zero mean input[1]

$$x(t) = z(t) - \lambda, \tag{3}$$

where $z(t)$ is a Poisson train of Dirac delta functions with mean rate λ, it can be shown that the functionals, G_i, in (2) are mutually orthogonal in the sense of time averages; namely,

$$E\{G_i \cdot G_j\} = 0 \qquad i \neq j,$$

where $E\{\ \}$ denotes expected value (Krausz, 1975). Furthermore, because $z(t)$ is a train of delta functions, no information about the system (1) is lost by excluding integrations along kernel diagonals since these integrations only produce lower-order functionals (Krausz, 1975). For an intuitive justification of this mathematical result see Krausz (1976).

Analogous to the Lee-Schetzen method for computing Wiener kernels, the kernels of (2) are found by input-output cross correlation;

$$h_n(\tau_1, \ldots, \tau_n) = \frac{1}{n!\lambda^n} E\{y(t)x(t - \tau_1) \ldots x(t - \tau_n)\}, \tag{4}$$

$$\tau_i\text{'s distinct.}$$

By substituting (3) for $x(t)$, the formulas for the first few kernels become

$$h_0 = E\{y(t)\}$$

$$h_1(\tau) = \frac{1}{\lambda} E\{y(t)z(t - \tau)\} - h_0$$

$$h_2(\tau_1, \tau_2) = \tfrac{1}{2}\left[\frac{1}{\lambda^2} E\{y(t)z(t - \tau_1)z(t - \tau_2)\}\right] \\ \left[-h_1(\tau_1) - h_1(\tau_2) - h_0\right] \tag{5}$$

$$\tau_1 \neq \tau_2.$$

Once the kernels of a system are known, series (2) allows prediction of the output in response to any impulse train input $z(t)$, but unless the kernels of all orders are known to perfect accuracy, the output of (2) will differ from the actual system output. However, due to orthogonality, when series (2) is truncated after n terms, its output gives the best

[1] Note that series (2) expresses the output of a point process system in terms of the signal $x(t)$ even though the actual input delivered to the system is represented by the impulse train $z(t)$. Of course (2) can be written in terms of $z(t)$ by using substitution (3).

nth order approximation to the Poisson train response of the actual system in the sense of minimum mean square error (MSE). Due to the statistical nature of this error criterion, it is impossible to know a priori the error that will result when a truncated series (2) is used to predict the response of a system when tested with a specific impulse pattern. Yet the fact that (2) minimizes the MSE implies the following trade-off. Series (2) rather accurately fits the system responses to input impulse patterns that are likely to be closely mimicked by a Poisson train with mean impulse rate λ, but the predicted response to an impulse pattern that would rarely occur (for example, two very high frequency bursts with a long gap in between) is less likely to be accurate. For a more quantitative discussion of this issue see Palm and Poggio (1977).

When one is attempting to analyze a point-process input system using Poisson stimulation, it is sometimes possible to save time and effort by incorporating into the analysis procedure any prior knowledge about the behavior of the system. In the present case, the fact that every PSP has the same time course allows the analysis to be simplified considerably. As might be expected, it is possible to use just the peak amplitude of each PSP, rather than the entire continuous intracellular potential, when calculating kernels.

Let $g(t)$ be the shape of a standard PSP and let $F(t_i)$ be the ratio between the amplitude of the i_{th} PSP and the standard. The intracellular potential in cell 3 (system output) in response to a train of presynaptic impulses is then

$$y(t) = \sum_i F(t_i)g(t - t_i). \tag{6}$$

If we now define a continuous function $F(t)$ and consider the values $F(t_i)$ to be samples of $F(t)$, then $F(t)$ itself can be expanded in a restricted diagonal series (2). In terms of the system kernels, $h_i(\tau_1, \ldots, \tau_i)$, the kernels of $F(t)$ are (Krausz and Friesen, 1975):

$$k_{i-1}(\sigma_1, \ldots, \sigma_{i-1}) = \frac{i!h_i(\sigma_1 + L, \ldots, \sigma_{i-1} + L, L)}{g(L)} \qquad i = 1, 2, \ldots \tag{7}$$

where L is the delay from stimulus pulse to PSP peak.

Together with $g(t)$ these kernels (k_i's) also serve to characterize transmission at the synapse. Thus, one argument in each system kernel may be fixed equal to the time delay between stimulus pulse and resulting PSP peak, thereby reducing by one the necessary dimensions of each kernel.

Experimental

Experiments were performed on the excised cardiac ganglion of a California spiny lobster (*Panulirus interruptus*). For a description of the dissection see Hartline (1967). The axon of cell 6 was stimulated extracellularly by a suction electrode and the intensity of stimulation was gradually increased until each stimulus pulse evoked a single EPSP in cell 3. Cell 3 PSPs were recorded by a microelectrode, amplified, displayed on an oscilloscope, and stored on FM magnetic tape. To eliminate spontaneous firing in the ganglion, all cells were hyperpolarized by use of a low K^+ Ringer's solution. This appeared to have little effect on the cell 3 PSP train evoked by cell 6 stimulation (Friesen, 1975). For a thorough discussion of experimental methods see Friesen (1975).

Poisson Stimulation

Pseudorandom numbers were generated by computer, one every 0.3 ms. If the random number was between 0.9990 and 1.0 a pulse was generated; otherwise no pulse. In this manner, a binary pseudorandom train of pulses was generated with a mean pulse rate of 3.3/s. Each pulse then triggered a Grass S-88 stimulator (Grass Instrument Co., Quincy, Mass.) which in turn shocked the cell 6 axon, evoking a single nerve impulse. Since the

0.3-ms binwidth of the pulse train is very brief compared to the time course of the synaptic facilitation and antifacilitation, and also compared to the decay constant of the PSPs themselves, the binary pseudorandom pulse train approximated adequately a Poisson process. The choice of mean impulse rate, λ, was a subjective one. With $\lambda = 3.3$/s, the mixture of short and long intervals in the Poisson train optimally explored the ranges of both facilitation and antifacilitation.

Data Acquisition and Storage

The continuous intracellular potential from cell 3 and the random pulse stimulus were recorded on separate channels of an FM tape. The continuous data were then low-pass filtered with a high cutoff of 320 Hz and digitized at a sampling rate of 1 kHz. The input impulse train was recorded by specially marking sampled output data points whenever a stimulus pulse occurred during the 1-ms time bin of the sample. The binwidth of the Poisson input was thus set equal to the sampling interval. A computer program measured the peak amplitudes of each PSP (the values of $F(t_i)$ in [5]) and stored these values along with information about the time of occurrence (t_i) of the immediately preceding stimulus pulse. The delay L between stimulus pulse and EPSP peak was quite constant as was the nearly exponential shape of each PSP. Therefore, when the entire continuous cell 3 output was needed, it was represented by a train of exponentially decaying pulses as in (6). The actual cell 3 EPSP waveform was fit by the function

$$g(t) = \begin{cases} e^{-(t-L)/\tau}, & t \geq L \\ o \qquad\quad , & t < L, \end{cases}$$

with $\tau = 20$ ms. For simplicity, L was normally set to zero. This representation of the continuous experimental output required very little storage space and had the additional advantages of lack of stimulus artifacts and base-line drifts.

Kernel Computation

Kernels were computed from input-output cross correlations according to (5), but with a slight modification due to the fact that $x(t)$ and $y(t)$ are actually finite length digitized signals. To illustrate, consider the expression for the second-order kernel. Since $z(t)$ is a train of impulses the expectation becomes

$$\begin{aligned} \frac{1}{\lambda^2} E\{y(t)z(t-\tau_1)z(t-\tau_2)\} &= \frac{1}{\lambda^2 T}\int_0^T y(t)z(t-\tau_1)z(t-\tau_2)dt \\ &= \frac{1}{\lambda^2 T}\int_0^T \sum_{i=1}^{N}\sum_{j=1}^{N} y(t)\delta(t-t_i-\tau_1)\delta(t-t_j-\tau_2)dt \\ &= \frac{1}{\lambda^2 T}\sum_{i=1}^{N}\sum_{j=1}^{N}\{y(t_j+\tau_2)\delta[(t_j-t_i)-(\tau_1-\tau_2)]\}, \end{aligned} \tag{8}$$

where N = number of impulses in time T and

$$\delta(t) = \begin{cases} 1/\Delta T, & t = 0, \text{ where } \Delta T \text{ is the binwidth.} \\ 0, & t \neq 0 \end{cases}$$

The final result in (8) denotes the sum of all y values that occur τ_2 s after the second member of each pair of impulses $(\tau_1 - \tau_2)$ s apart. The sum is formed over all such pairs, regardless of intervening impulses, and is then divided by $\lambda^2 T\Delta T$.

Rather than being divided by $\lambda^2 T\Delta T$, each sum of y values was instead divided by the number of impulse pairs contributing to that sum, yielding simply the average output that follows all impulse pairs with a given separation. This alternate procedure is

preferred for the following reason. In a train of N impulses there will be approximately $N\lambda\Delta T$ pairs of any given separation $(\tau_1 - \tau_2)$ since, for each of the N impulses in the train, the probability of another impulse occurring $(\tau_1 - \tau_2)$ s later is $\lambda\Delta T$. But with a mean impulse rate of λ,

$$N \approx \lambda T$$

$$N\lambda\Delta T \approx \lambda^2 T\Delta T.$$

Therefore in the limit as experimental time approaches infinity, both kernel estimation procedures converge to the same result. However, for small numbers of input impulses, the difference between the actual number of pairs with a given separation and $\lambda^2 T\Delta T$ accounts for an appreciable amount of the statistical fluctuation in a kernel estimate.

After kernels had been computed by the method above, enough noise remained in the higher kernels to warrant a certain amount of smoothing. For two-dimensional kernels, first the rows and then the columns of the kernel matrix were smoothed with a "hanning" window (Blackman and Tukey, 1959). This smoothing operation was repeated as often as deemed necessary, taking care to avoid the introduction of significant distortions. The entire kernel computation procedure was tested and verified by using a known simulated second-order nonlinear system (Krausz, 1976).

Prediction of Output from Kernels

Given the system kernels, (2) allows prediction of the output in response to any impulse train input. In this study the system kernels were computed according to (5) and (8) with one argument in the highest kernel held fixed. Then the resulting kernels of $F(t)$ from (7) were used in (2) to predict values for $F(t_i)$. After $z(t) - \lambda$ has been substituted for $x(t)$ in (2) most of the integrals become summations, so the computation proceeds quite rapidly. From the predicted values of $F(t_i)$ the continuous system output is easily reconstructed by using (6).

RESULTS

Kernels up to third order describing the effect of cell 6 stimulation on the postsynaptic potential recorded from cell 3 were computed from 18 min of experimental data. As explained under Materials and Methods (Data Acquisition), each PSP was replaced by an exponentially shaped pulse with the same amplitude. The first-order kernel (Fig. 1) resembles an exponential pulse except for the slight undershoot at about 100 ms. Since the output after every presynaptic impulse is averaged to compute $h_1(\tau)$ using (5), this undershoot reflects the fact that PSPs after the second of a pair of impulses 100-ms apart tend to be antifacilitated and contribute less than normal to this average (Krausz, 1975).

Fig. 2 displays the values of the second kernel, $h_2(\tau_1, \tau_2)$, for all values of τ_1 and τ_2 such that $0 < \tau_2 < \tau_1 < 2$ s. Since the kernel is symmetric about the diagonal, values of $h_2(\tau_1, \tau_2)$ for $\tau_1 < \tau_2$ are redundant and are omitted from the figure. After the second kernel had been computed according to the procedure described in Materials and Methods, a hanning smoothing window was applied twice, alternately, to the rows and columns of the kernel matrix.

The main features of Fig. 2 appear in the first line of the plot, where $\tau_2 = 0$. The values of $h_2(\tau_1, \tau_2)$ describe the average facilitation or antifacilitation of response peaks after the second of a pair of impulses. When τ_1 is less than about 200 ms, the second kernel becomes negative, indicating antifacilitation. For τ_1

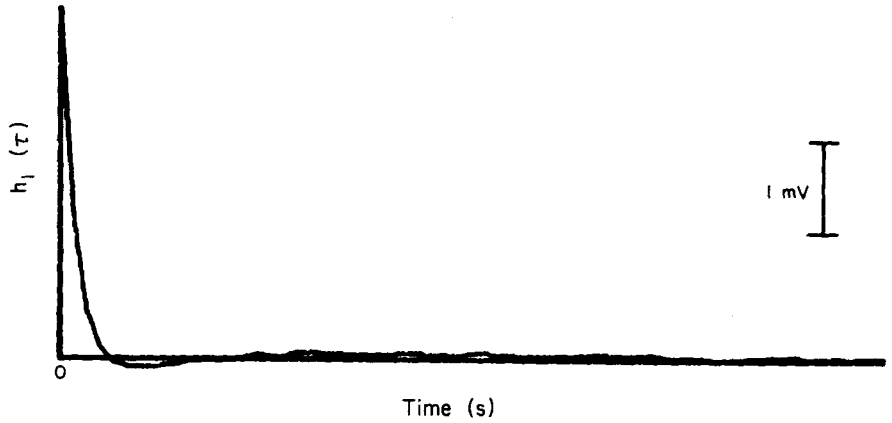

FIGURE 1. Experimental first kernel. This estimate of the first kernel was computed from 18 min of cell 3 response during Poisson stimulation of the cell 6 axon.

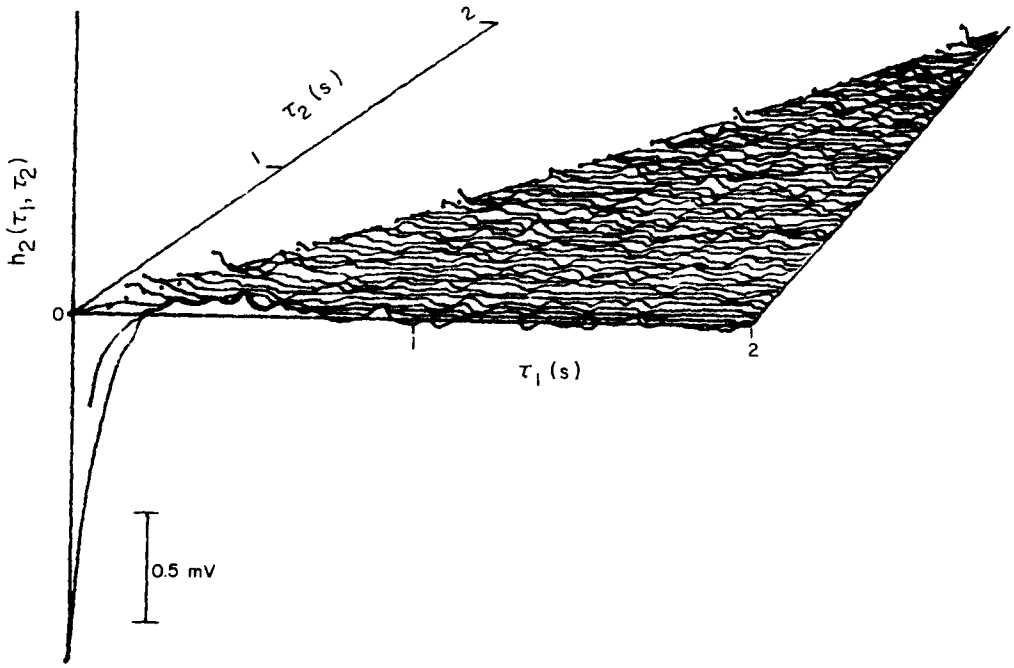

FIGURE 2. Experimental second kernel. Each line in the figure represents values of the second kernel, $h_2(\tau_1, \tau_2)$, for a fixed value of τ_2. Between successive lines, τ_2 is incremented by 32 ms. This kernel was estimated from 18 min of experimental Poisson train response. The figure uses hidden line suppression and perspective. Only one diagonal half of the symmetric kernel is shown.

values between about 200 and 400 ms there is a very slight facilitatory peak in $h_2(\tau_1, \tau_2)$. For larger values of τ_1 and τ_2, the second kernel becomes negligible.

Fig. 3 shows values of the third-order kernel, $h_3(\tau_1, \tau_2, 0)$, with $\tau_3 = 0$. Due to the simplification provided by (7), other values of τ_3 need not be considered.

After the third-order kernel had been calculated from EPSP peaks only, the rows and columns of the resulting two-dimensional matrix were smoothed four times alternately with a hanning window. Again due to symmetry, only values of $h_3(\tau_1, \tau_2, 0)$ for $\tau_1 > \tau_2$ are shown in Fig. 3. Since there are fewer impulse triplets of each configuration in the 18-min Poisson input than there are impulse pairs, the third kernel estimate has considerably more variance than does the estimate of the second kernel in Fig. 2. In spite of this "noise" certain features of the third kernel are readily apparent. Starting at the origin and moving along the diagonal, Fig. 3 shows that whenever a closely spaced impulse pair occurs, the EPSP

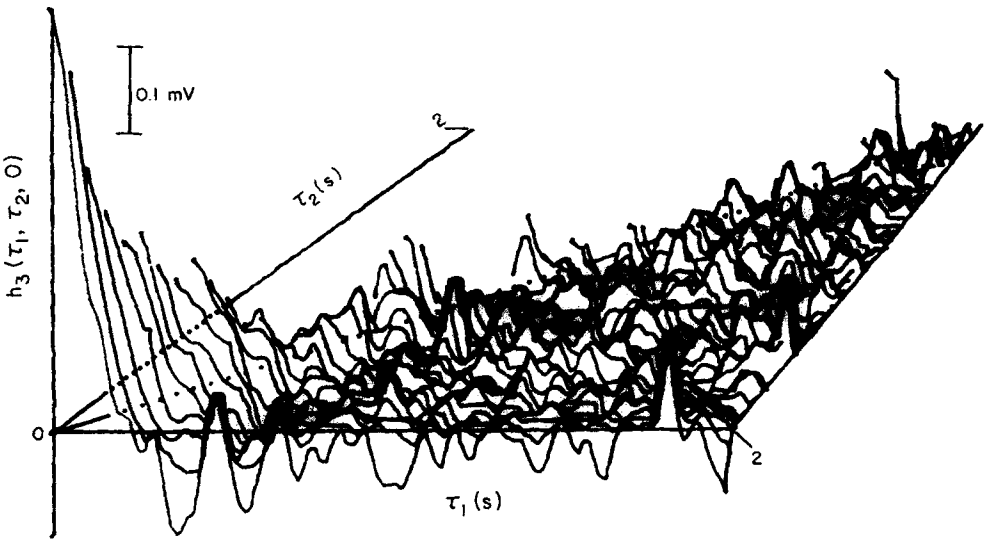

FIGURE 3. Experimental third kernel. Each line in the figure indicates the value of $h_3(\tau_1, \tau_2, 0)$ for a fixed value of τ_2. Between successive lines, τ_2 changes by 32 ms. Values of the third kernel were estimated from 18 min of experimental PSP peaks. Experimental third kernel is much noisier than the second kernel in Fig. 2. The figure uses hidden line suppression and perspective.

after a third impulse is larger, on the average, than would be predicted from second and lower kernels only. The amount of this third-order augmentation following closely spaced pairs decreases as the third impulse moves farther away from the pair. Moving away from the diagonal, there is also a decline in the third kernel amplitude as the pair separation, $\tau_1 - \tau_2$, is increased. This decline leads into a shallow valley of decreased response amplitude for $\tau_2 < 1$ s and $\tau_1 < 500$ ms.

Output Calculated from Kernels

On the basis of the first kernel only, series (2) approximates the cell 3 output with a train of identical exponentially decaying pulses. With $g(t) = \exp(-t/\tau)$, the constant pulse amplitude determined from (7) is $k_0 = h_1(0)$. The MSE between cell 3 postsynaptic potential output and first-order approximation is 19% of the total power in the continuous cell 3 signal (Krausz, 1976).

When the second-order functional in (2) is added to the approximation, predicted PSPs begin to show some variability. Due to the negative peak in $h_2(\tau_1, \tau_2)$ (Fig. 2), the predicted PSP amplitude after a pair of closely spaced impulses will be antifacilitated. Very little facilitation of PSPs is expected from Fig. 2. From (7), (2), and (6) the second-order nonlinear approximation to the Poisson train response of the synapse was calculated for comparison with the actual response. Fig. 4 compares 2,000 second kernel predicted PSPs with the actual PSPs resulting from Poisson stimulation. Each dot in the scatter diagram gives predicted vs. actual PSP amplitude for a single PSP from the random train. In the case of a perfect fit all the points would lie along the diagonal.

Obviously, the second-order prediction is far from perfection, but it is a significant improvement over the first kernel (linear) approximation. Given only the first kernel, all points in the scatter diagram (Fig. 4) would fall along a horizontal line. Instead, small experimental PSPs are approximated by small predicted PSPs although the amount of antifacilitation predicted by $h_2(\tau_1, \tau_2)$ is generally insufficient. In some cases, however, too much antifacilitation leads to a number of negative amplitude predicted PSPs in Fig. 4. Even though no information about the temporal ordering of PSPs appears in the scatter diagram, it is safe to say that negative predicted PSPs arise in cases where three input impulses are so closely grouped that the summed antifacilitation contributed by each of the first two impulses (via the second kernel) causes the amplitude of the third PSP to be underestimated. The positive peak near the origin in the third kernel (Fig. 3) serves to counteract this excess depression.

Fig. 4 also reveals the lack of sufficient facilitation in the second kernel approximation. Large experimental PSPs are consistently underestimated. Overall, the MSE between kernel predicted and actual PSP amplitudes is nevertheless reduced to 9.5% by the addition of the second-order kernel.

Due to the orthogonality of (2), addition of the third-order functional should improve the accuracy of the predicted output. After the effect of the third kernel (Fig. 3), had been added in the scatter diagram of Fig. 5 was produced. Two observations are immediate when Fig. 5 is compared with Fig. 4. First, the points do tend to distribute more about the diagonal. The kernels now predict an appreciable amount of facilitation, improving the fit to large experimental PSPs. Second, there is a great deal of scatter in the predicted PSP amplitudes, somewhat more scatter than is observed in Fig. 4. This increase in scatter must be partly attributed to the noisiness of the experimental third kernel (Fig. 2).

On the basis of all the kernels up to third order, the MSE between predicted and actual PSP trains was again 9.5%. So addition of the third kernel contribution did not improve the fit. This result is not surprising since there is no guarantee that the third-order functional computed from a noisy estimate of the third kernel will be orthogonal to the lower-order functionals.[2] With a data sample larger than 18 min, the input statistics will more nearly approximate the ideal Poisson case, so better resolution of the third kernel and improved predic-

[2] In their analysis of catfish horizontal cell responses, Marmarelis and Naka (1973*b*) actually found a considerable increase in the MSE when the effects of a noisy third kernel estimate were added to their second-order prediction of output.

tion of output should result. This claim is substantiated by the analysis of a model of the synapse presented in the next section.

DISCUSSION

The results indicate that a Poisson train analysis can yield an accurate characteri-

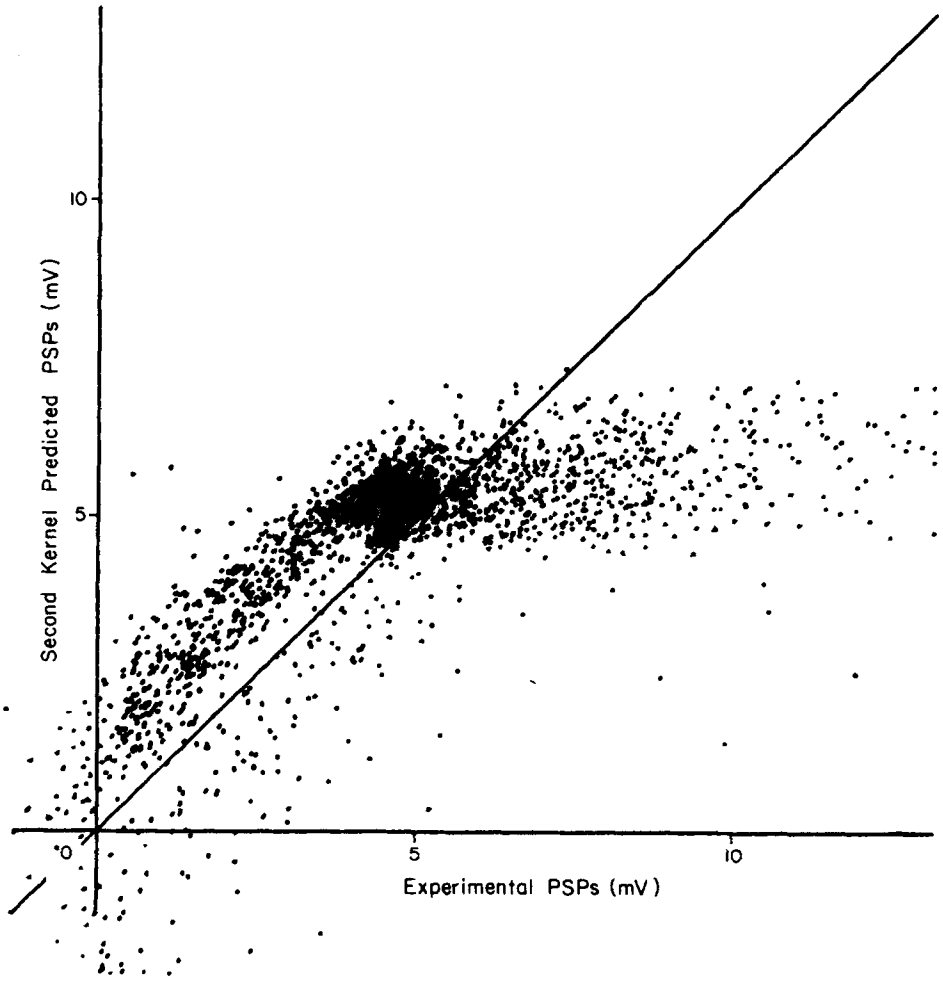

FIGURE 4. Scatter diagram comparison of experimental PSPs and PSPs predicted from experimental kernels up to second order. Both synapse and kernel model were tested with same Poisson impulse train input. Each of the 2,000 points in the figure indicates kernel predicted and experimental amplitudes for corresponding PSPs. If the kernels up to second order characterized the experimental output with perfect accuracy, then all points would lie along the diagonal line.

zation of transmission at a nonlinear synapse. So the answer to the first of the questions raised in the introduction is "yes," although it is apparent from Fig. 5 that more data would be helpful in the case of the lobster cardiac ganglion synapse. With a long enough data sample, the variance of the third kernel

estimate could be decreased and the scatter of points in Fig. 5 would be reduced. The kernel prediction would improve further in accuracy if a reasonably noise-free fourth kernel could also be measured.

Estimation of a fourth kernel, even when one argement is held fixed, requires

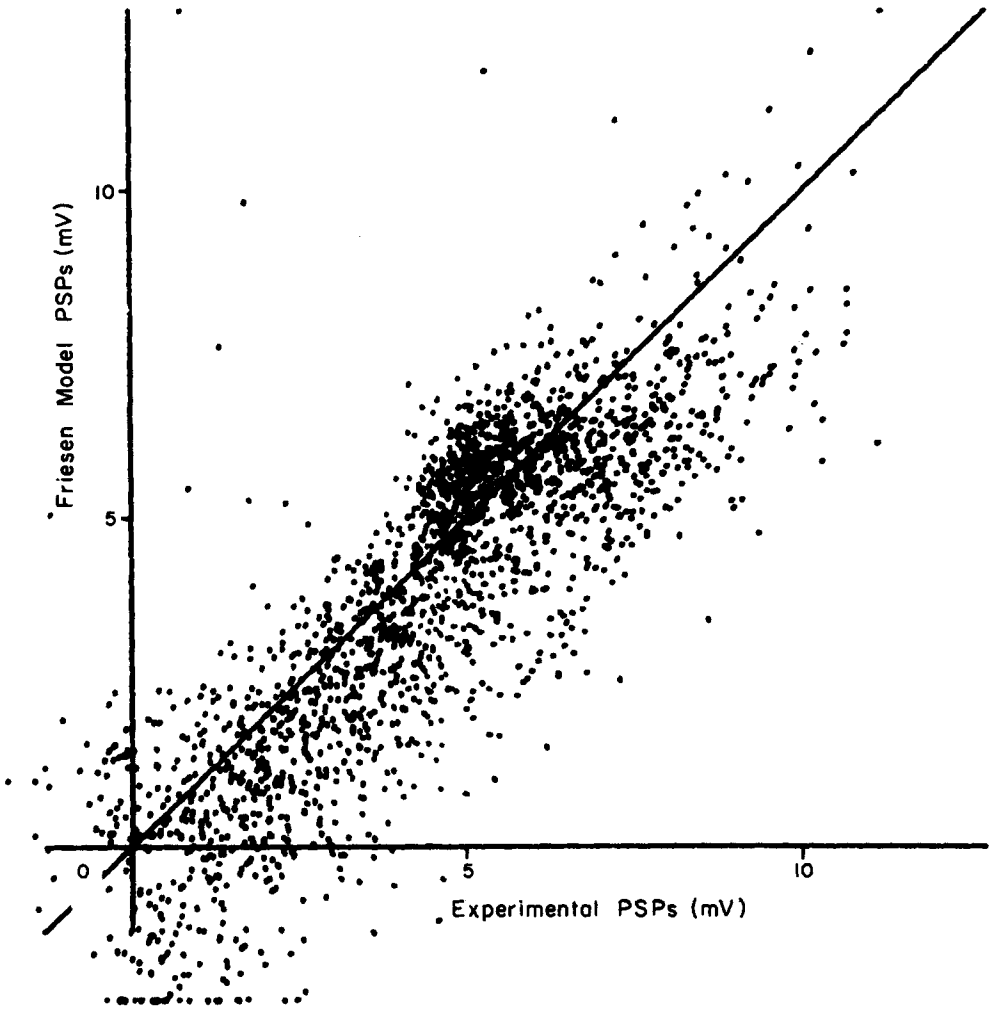

FIGURE 5. Scatter diagram comparison of experimental PSPs and PSPs predicted from experimental kernels up to third order. Both the experimental preparation and the kernel model were presented with the same Poisson impulse train input. Each of the 2,000 points in the figure indicates kernel predicted and experimentally measured amplitudes for corresponding PSPs.

a tremendous sample of data and much computation. Fortunately, third-order kernels are sufficient for many biological systems, partly because of the linearizing effects of intrinsic noise (Marmarelis, 1975; Krausz, 1976). Since kernels higher than third order are apparently required to characterize transmission at

the cardiac ganglion synapse, it seems that this is one of the more difficult systems to analyze by the Poisson impulse train method.

To illustrate this point by means of a comparison, consider transmission at the magnesium-blocked frog neuromuscular junction. There, facilitation of end-plate potentials (EPPs) has been described as a linear function of input comprising two or perhaps three components (Mallart and Martin, 1967; Magleby, 1973*a*). Systems displaying linear facilitation have only second and lower kernels (Krausz and Friesen, 1975). To account for the effects of repetitive stimulation on the end-plate potential, Magleby (1973*a*, *b*) and Magleby and Zengle (1975*a*, *b*) propose a multiplicative factor, "potentiation," which will cause the model kernels to depend on the mean rate of Poisson stimulation, but will probably not increase the order of the model much beyond second order for any given value of λ.

Other authors (Dodge and Rahamimoff, 1967; Younkin, 1974) have suggested that EPP amplitude is proportional to the third or fourth power of a linear function of input (presumed to represent the accumulation of residual calcium in the axon terminal). By raising a first-order series (2) to the third or fourth power, it is easy to see that only kernels up to third or fourth will result.

Since these various models have had reasonable success at fitting the end-plate potential amplitudes after junctional stimulation with various impulse patterns, it is likely that a third-order series (2) would characterize frog neuromuscular transmission rather well. Unfortunately, no model of the neuromuscular junction (NMJ) has been tested with a wide variety of impulse patterns, as occurs during Poisson stimulation, so it is not known how accurately such models, with their chosen parameter values, are able to account for the responses to input patterns different from those which were used to construct the models in the first place.

In order to make a comprehensive comparison between this traditional try-and-cut modeling approach and the Poisson train analysis method, a mathematical model of the cardiac ganglion synapse (Friesen, 1975) was challenged with the same sample of Poisson white noise used to characterize the living synapse. Before discussing model predictions it is worthwhile to review briefly the experiments and assumptions from which the model was derived.

The Friesen Model

To study nonlinear transmission at the cell 6-cell 3 synapse, Friesen (1975) stimulated the cell 6 axon with closely spaced volleys of from one to four shocks followed at a variable time interval by a test shock. With facilitation, F, defined as the ratio between the amplitude of the EPSP evoked by the test shock and the amplitude of the first EPSP during the conditioning volley, Friesen plotted the curves in Fig. 6 for facilitation as a function of time interval. Notice that for any value of t in Fig. 6, the F vs. t curves for different numbers of conditioning impulses, N, are nearly equally spaced. Friesen therefore assumed that F is the sum of two components: a facilitation component, F^+, that is proportional to N; and an antifacilitation component, F^-, independent of N. Altogether then

$$F(N, t) = F^+(N, t) + F^-(t),$$

where

$$F^+(N, t) = N \cdot F_1^+(t),$$

and F_1^+ is the facilitatory effect of each impulse in the conditioning volley. To test further the linear dependence of F on N, Friesen fixed t = 800 ms and varied N from 1 to 10. In several experiments F rose linearly with N for small values of N (four or less) and then began to level off.

From the data in Fig. 6, $F_1^+(t)$ was determined by averaging the differences between the curves for different values of N. Then $N \cdot F_1^+$ was subtracted from F

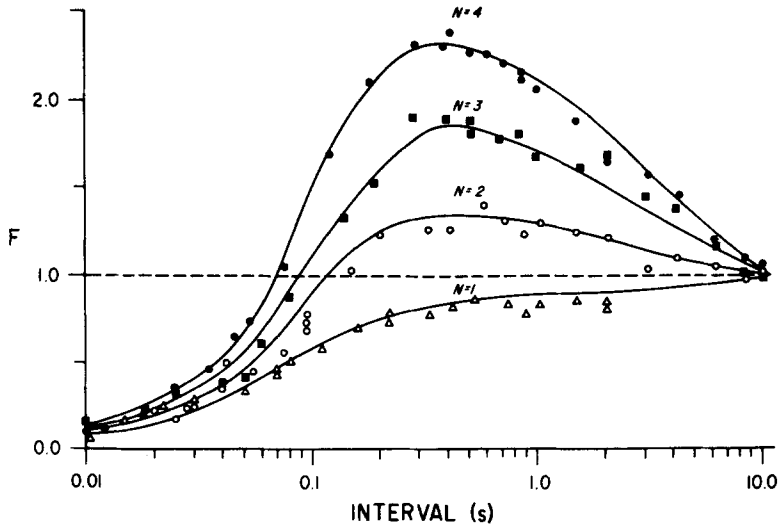

FIGURE 6. Results of Friesen's conditioning volley-test stimulus experiments. The time interval between the conditioning volley and the test stimulus is plotted along the abscissa in log units. The amplitudes of PSPs evoked by the test impulse are expressed as a fraction, F, of the unconditioned PSP amplitude. Each discrete point represents data from an experiment with N = 1, 2, 3, or 4 conditioning impulses. The four solid lines indicate F values predicted by the Friesen model and the dashed line denotes the value of F for an unconditioned PSP. (Reprinted from Friesen [1975] with permission of Springer-Verlag.)

to estimate F^-. Using data from four different experiments, Friesen found that F_1^+ varied between experiments while F^- remained quite consistent. The curves for F_1^+ and F^- were fit closely by the expressions

$$F_1^+ = Ce^{-t/3.6}\,(1 - e^{-t/0.08})^2,$$
$$F^- = 1.0 - 0.26\,e^{-t/0.02} - 0.74\,e^{-t/4.1},$$

where C is a constant with a different value for each experiment and t is time in seconds.

To give these expressions a mechanistic interpretation, Friesen proposed that the amount of transmitter released by each presynaptic impulse is the sum of contributions from two compartments, A and B (Fig. 7). Both compartments are

emptied by the occurrence of an impulse and then begin to refill. Compartment A fills according to the expression for F^- with t equal to the time since the most recent impulse. To account for F^+ and its linear dependence on N, let each presynaptic impulse cause a hypothetical pool D to be incremented by a fixed amount of transmitter. Let the contents of D leak into another pool C which in turn decays into B and assume that B itself is leaky. Then by assigning the proper rate constant to each decay process, Friesen arrived at the equation for F_1^+.

Tests of the Model

Though designed to account for the results of conditioning volley test stimulus experiments (Fig. 6), the Friesen model is complete enough to allow testing with

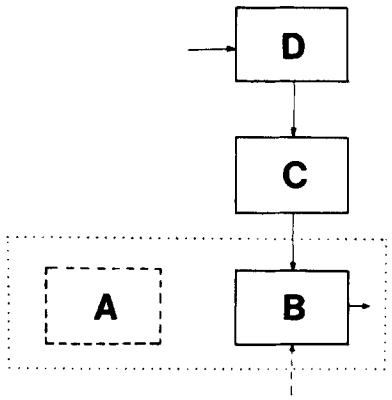

FIGURE 7. Diagram of Friesen's hypothesized transmitter pools. Pool D is incremented by a fixed amount immediately after each input impulse. At the same time, all of the transmitter in both the A and B pools is released, causing a PSP in cell 3 whose amplitude is proportional to the amount released. In the modification suggested in the discussion pool A is eliminated and instead, pool B undergoes a constant filling. The rate of filling is incremented transiently after each impulse.

any stimulus pattern. The preferred stimulus for comparing model performance with experimental results is white noise. White-noise inputs provide an objective and comprehensive comparison, since they randomly present a wide variety of test patterns. Therefore, to answer question (*b*) in the Introduction, the model was computer simulated and presented with the same 3.3/s Poisson impulse train that was used in the experimental analysis of the living synapse.

The model PSP amplitudes are compared with experimental values in the scatter diagram of Fig. 8. Model responses were scaled to minimize the MSE between model and experiment. From the figure it is obvious that the model is quite accurate, particularly for PSPs in the range of about 1–5 mV amplitude. There is more scatter in model predictions for PSPs larger than 6 mV, but the points still distribute evenly around the diagonal, indicating that the errors in model performance are not consistently biased toward undersized or oversized PSPs. The model does tend to underestimate the amplitude of experimental

PSPs in a small amplitude range around 5 mV. For some unknown reason, a great cluster of points appears just below the diagonal (Fig. 8) with model PSP amplitudes all around 4 mV. Near the origin the experimental PSP values are slightly unreliable, and negative experimental PSPs are known to be an artifact

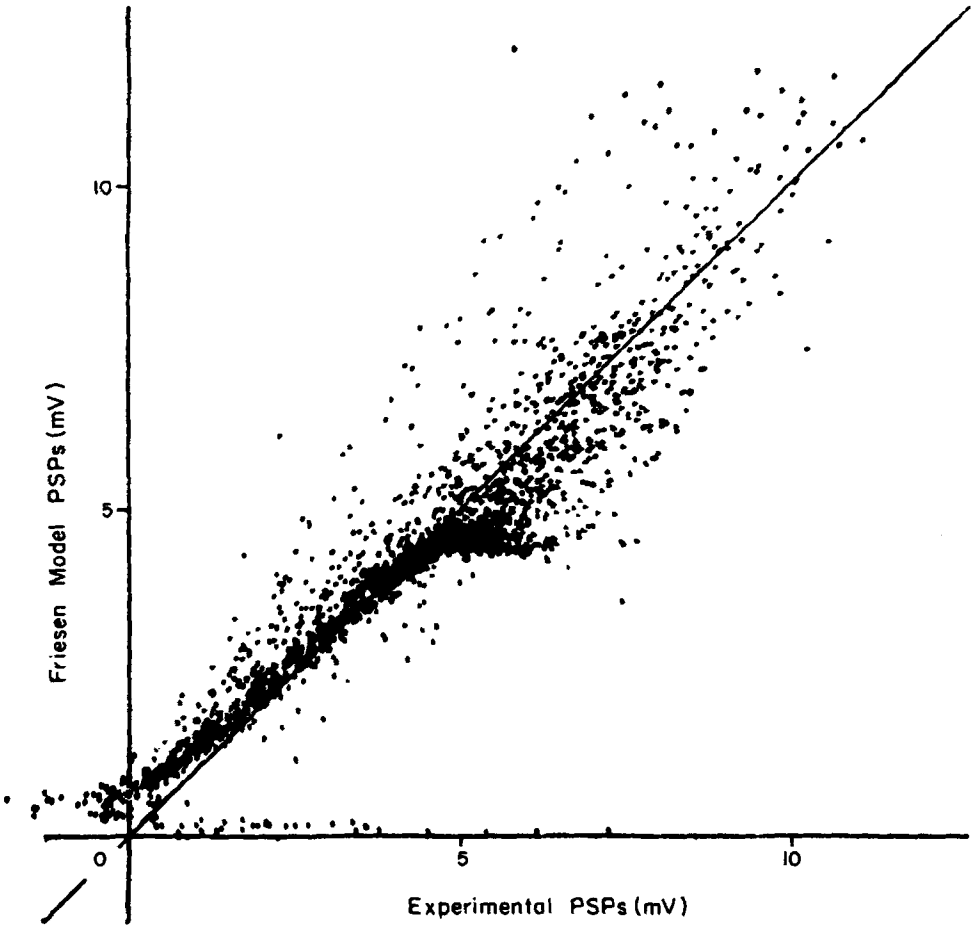

FIGURE 8. Scatter diagram comparison of Friesen model and experimental data. Both model and ganglion were presented with the same Poisson impulse train. The coordinates of each of the 2,000 points in the figure indicate model amplitude and experimental amplitude for corresponding PSPs. If model predictions were perfectly accurate, all points would lie along the diagonal line.

of the data acquisition procedure (Krausz, 1976). Overall, the MSE between experiment and model based on 3,000 randomly occurring PSPs was 4%. Therefore, in answer to question (*b*) of the Introduction, the model is significantly more accurate than the three-kernel characterization derived from 18 min of Poisson stimulation.

As mentioned earlier, the scatter diagram method of comparison ignores all

information about PSP timing. The only complete way to compare model predictions with actual cell 3 output, other than by directly comparing the entire continuous output signals, is to compare model kernels with experimental kernels. If noise is present in the experimental output, a comparison of kernels is preferable to a comparison of output signals, since output noise uncorrelated with input is averaged away during kernel computation.

It would be convenient if the model kernels could be calculated analytically by somehow manipulating the model equations into the form of a restricted diagonal series (2). The kernels would then be known by inspection. Since the F^+ component in the model depends linearly on input impulses, it would seem that a second kernel would characterize at least the facilitation if not the depression. However, the hypothesized emptying of both transmitter pools A and B introduces a strong nonlinearity. This resetting feature also makes it impossible to write the model as a closed-form expression giving output as a function of input, so analytic calculation of the kernels by inspection is ruled out.

Another approach (not as appealing) is to try to calculate kernels analytically by using the known statistical properties of a Poisson process in conjunction with the cross-correlation formulas (5). Specifically, the first kernel is found from the expected levels of "transmitter" in pools A and B. The second kernel involves conditional expectations dependent upon impulse pairs, and these lead to rather complicated subcases. Although this method has successfully been used to calculate the kernels of one resetting type nonlinear system (Krausz, unpublished results), it seems unlikely to work for the Friesen model. Thus computer simulation and testing of the model is inescapable.

The second kernel of the Friesen model is shown in Fig. 9. It was calculated from 5.5 h of model-generated output in response to a 3.3/s Poisson train input, and has been smoothed twice with a hanning window. There is slightly more facilitation in the model second kernel than in the corresponding experimental kernel (Fig. 2), reflecting some consistent difference between model and experiment. The third-order kernel (Fig. 10) shows basically the same features as the experimental third kernel (Fig. 3), but is far less noisy. Without more experimental data it is difficult to say whether or not significant differences exist between model and experimental third kernels.

Since model kernels are so similar to experimental ones, the model kernels can be used to estimate the accuracy that would have resulted from a third-order characterization of the experimental system given better resolution of the experimental third kernel. Fig. 11 is a scatter diagram comparison of model output and model output predicted from model kernels up to third order. As expected, Fig. 11 looks very similar to the corresponding scatter diagram for the experimental system (Fig. 5) and the dots are less widely scattered. On the basis of 3,000 responses, the MSE between model output predicted from kernels and known model output is 6.5%. Given sufficient resolution of experimental kernels, the MSE between kernel predicted and actual experimental output would therefore be about 6.5%, rather than the 9.5% determined from 18 min of data. A summary of MSE values for all the various comparisons between output signals appears in Table I.

White-Noise Analysis or Educated-Guess Modeling

To answer the third question in the Introduction about the comparative efficiency and respective advantages of the white-noise and modeling approaches it is necessary to know how much time was involved in devising a model. If fully automated, the conditioning volley test stimulus results in Fig. 5 could have been obtained in about 4 h, but these results alone do not allow prediction of output in

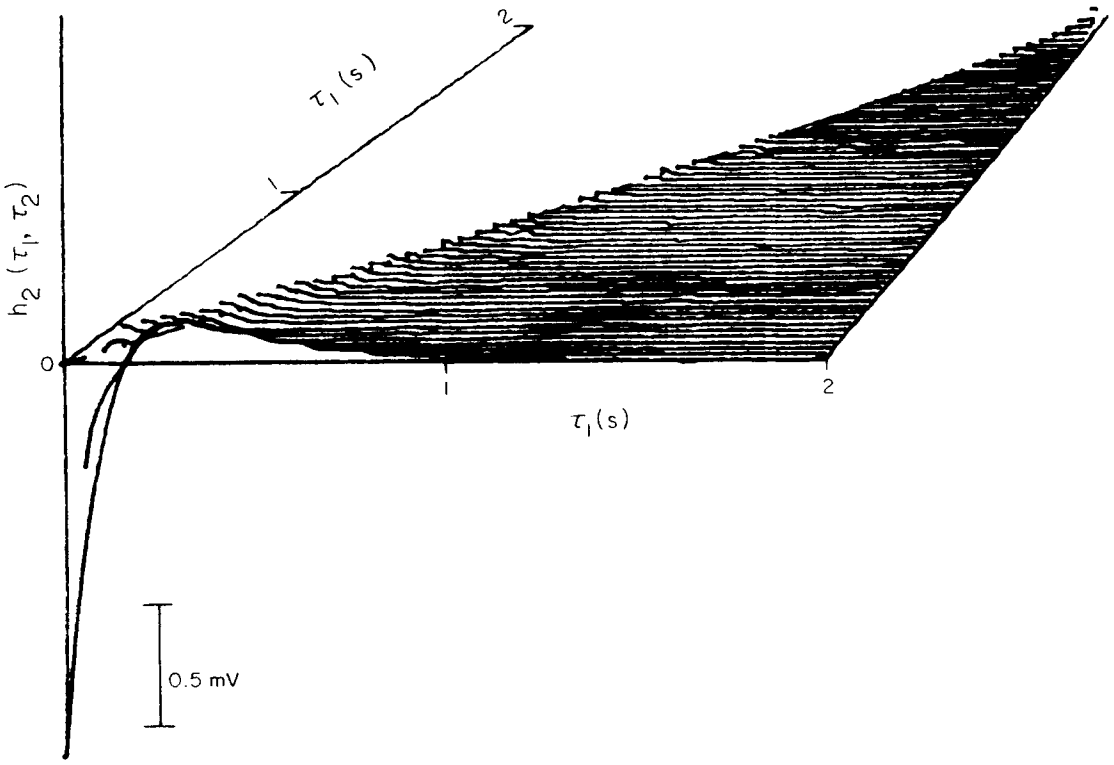

FIGURE 9. Model second kernel. Each line in the figure represents values of the second kernel, h_2 (τ_1, τ_2), for a fixed value of τ_2. Between successive lines, τ_2 is incremented by 32 ms. This kernel was estimated from 5.5 h of Friesen model-predicted Poisson train response. The figure uses hidden line suppression and perspective. Only one diagonal half of the symmetric kernel is shown.

response to arbitrary inputs. Many more hours and some ingenuity were required for the construction of a model. In its original version, pools A and B were not reset to zero after each impulse. More experiments using two test stimuli (Friesen, 1975) were required before the need for this added assumption was established. In contrast to the model-building approach, a reasonably accurate characterization of transmission at the cell 6-cell 3 synapse follows immediately from the results of one 5.5-h Poisson train experiment. So even in the highly nonlinear example of the lobster cardiac ganglion synapse, the Poisson

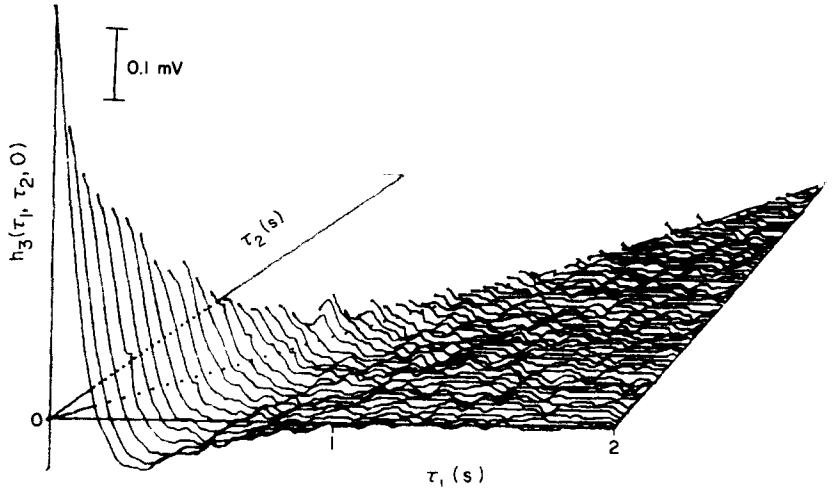

FIGURE 10. Model third kernel. Each line in the figure indicates the value of $h_3(\tau_1, \tau_2, 0)$ for a fixed value of τ_2. Between successive lines, τ_2 changes by 32 ms. Values of the third kernel were estimated from 5.5 h of simulated Friesen model output using only the PSP peaks. The figure uses hidden line suppression and perspective. Notice the reduced amount of statistical noise compared with Fig. 3.

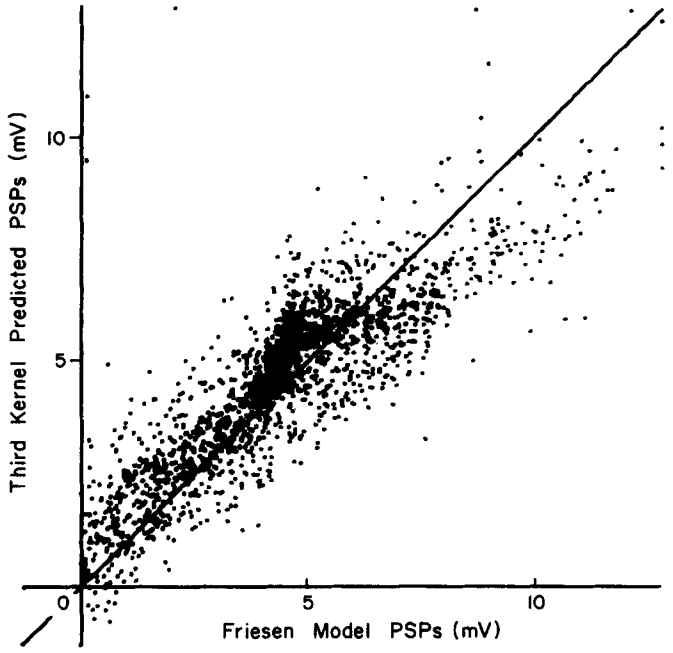

FIGURE 11. Scatter diagram comparison of Friesen model PSPs and PSPs predicted from model kernels up to third order. Both model and kernel predictions use the same Poisson impulse train input. Each of the 2,000 points in the figure indicates kernel-predicted and Friesen model-predicted amplitudes for corresponding PSPs. If the kernels up to third order characterized the Friesen model with perfect accuracy, then all points would lie along the diagonal line. Note the improvement in fit compared to Fig. 5.

train analysis is simpler and more efficient than model making.

Compared with other system analysis approaches, the Poisson train method shares the same advantages as the Wiener method for continuous-input systems. These are summarized below and discussed at greater length by Marmarelis and Naka (1973*a*, 1974).

(*a*) The experimental paradigm is simple to program and deliver.

(*b*) Since the mean rate of input impulses is constant, the state of adaptation of the system is controlled.

(*c*) Noise at the output uncorrelated with input is averaged out during kernel computation.

(*d*) The entire system analysis and synthesis procedure is known and does not depend on the particular system under study. Once the Poisson train response is recorded, the system is characterized by a set of input-output cross correlations (kernels) which allow prediction of output in response to arbitrary inputs.

(*e*) The analysis is objective, giving an overall fit to the noise response of the system, rather than a fit dependent upon a specific class of inputs such as sinusoids or steps.

TABLE I

SUMMARY OF MSE VALUES

	Experimental responses	Friesen model responses
	%	%
First kernel prediction	19	20
Second kernel prediction	9.5	10
Third kernel prediction	9.5	6.5
Friesen model	4	–

Calculated mean square errors as a percentage of total output power. The experimental synapse, experimental kernels, Friesen model, and model kernels were each presented with an identical 3,000 impulse Poisson train. When Friesen model output was compared with experimental output, the former was scaled so as to minimize the MSE.

The fourth and fifth advantages of the white-noise approach deserve special emphasis. The ability to predict input from output for arbitrary inputs is a built-in feature of the analysis technique. In contrast, three interrelated problems must be overcome before a conventional model can claim to do the same.

Normally, a model is initially designed to account for the responses a system gives to a restricted set of simple inputs (such as conditioning volleys followed by test impulses). Usually, the model will next need to be generalized before it can even be tested with inputs other than those used for its initial construction. (Friesen's curves for F_1^+ and F^- cannot be used directly for arbitrary impulse patterns. It was necessary to postulate the various transmitter pools and then to add the assumption about zeroing pools A and B after each impulse.) Third, a prospective model must be tinkered with and its parameters adjusted until it gives accurate predictions to all sorts of inputs including random inputs. Models in general suffer from the chronic malady that one set of parameters will be optimal for a given class of inputs but a different set of parameters works much better with other inputs. The global, minimum MSE fit produced by a Poisson

train analysis depends only on one parameter, the mean impulse rate. Perhaps models should be tested with white noise and their parameters adjusted to meet the same minimum MSE criterion.

If a model can be devised that accurately characterizes a system, it will then have at least two important advantages over a white-noise identification.

(*a*) If a limited set of test inputs can be used for the construction of a model that generalizes to all other inputs, then some simplifying property of the system will have been uncovered. As an example, Friesen was able to characterize the lobster cardiac ganglion synapse by applying constant frequency-conditioning volleys followed by test impulses. The simplifying property of the system that allowed his model based on these results to generalize to the Poisson input case was the fact that the facilitatory effects of each conditioning impulse on the test PSP added linearly.

(*b*) It is easier to suggest physiological mechanisms corresponding to the variables and parameters of a custom-built model than to a set of kernels. This is partly because an accurate model must exploit some simplifying property of the system, as explained in (*a*) above.

Another reason (for *b*) is simply that physiologists are more practiced in dealing with conventional as opposed to white-noise models. In the usual approach to modeling, experiments are designed to produce a set of curves, each describing the effect of one variable on another while others are held fixed. The resulting curves are then fit by exponentials which are interpreted as the build-up and decay of various quantities according to first- or second-order kinetics.

To make similar kinds of interpretations based on a set of kernels, it would be helpful to have a table of nonlinear devices and their respective kernels. Once a system's kernels were known, a search through such a table would suggest possible mechanisms. Another, more or less opposite approach is to use the kernels as a substitute for the actual system and to computer simulate conventional experiments. This allows construction of a more conventional model without the difficulties of performing each experiment on a living preparation. As a test of this approach, and to answer question (*d*) in the Introduction, an attempt was made to duplicate the results of Friesen's conditioning volley-test stimulus experiments (Fig. 6) by using measured kernels in place of the living synapse. Since model kernels are quite similar to experimental kernels and are much less noisy, this test was performed with model rather than experimental kernels. Although the resulting curves (not shown) did somewhat resemble those in Fig. 6, the linear dependence of $F(N, t)$ on N did not hold. Some discrepancy is not surprising in view of the fact that Friesen's conditioning volley-test stimulus paradigm is rarely imitated by a Poisson process and, as mentioned earlier (Materials and Methods), the error of a kernel response to a specific pattern depends on the frequency of occurrence of that pattern in the white-noise input.

Since the observation that $F(N, t)$ varies linearly with N (Fig. 6) was crucial to the development of his model, Friesen could not have constructed his model from three kernels estimated from 5 h of Poisson stimulation of the synapse. Given enough data to calculate a fourth kernel, perhaps Fig. 6 could be adequately replicated with kernels.

In the case of the lobster cardiac ganglion synapse, there is no need to develop a mechanistic model from kernels since the Friesen model already exists. However, in answer to the last question in the Introduction, the white-noise analysis still leads to insights about mechanism when model and actual response to white-noise stimuli are compared. As mentioned earlier, the Friesen model proved to be quite accurate when tested with Poisson trains, but there were a few consistent errors. An examination of the input impulse patterns that precede erroneous model predictions might suggest ways in which the model could be improved. For example, one possible simplification, one would hope an improvement, eliminates pool A entirely (Fig. 7). By assuming instead that pool B is steadily filled from some inexhaustible supply, and that the rate of filling is incremented transiently after each presynaptic impulse, it is possible to account for $F^{-}(t)$ without assuming a separate pool A (Krausz, 1976).

Once the Poisson train kernels of a modified version of the Friesen model agree with experimentally determined kernels, consistent errors in the model will disappear and our knowledge of the transmission properties of the synapse will be refined. By providing a standard of performance for models, white-noise analysis assists the search for underlying mechanisms.

SUMMARY AND CONCLUSIONS

Both a living synapse in the lobster cardiac ganglion and a mathematical model of nonlinear transmission at the synapse were tested with Poisson trains of impulses. Experimental results demonstrated that the transmission properties of the synapse can be characterized with reasonable accuracy by using kernels up to third order.

A comparison of experimental and model responses to Poisson stimulation demonstrated that the model is generally quite accurate, even though the model was constructed by testing the synapse with a rather restricted set of inputs.

There were some consistent differences between model predictions and actual synaptic output. These differences were reflected, at least in part, by a slight difference between experimental and model second kernels. In conclusion, the Poisson white-noise analysis technique is a useful and objective way to evaluate the performance of a custom-made model and, in addition, provides an arbitrarily accurate characterization of a system's properties even in complicated cases where other modeling approaches are inadequate.

The authors wish to thank Drs. G. D. Lange, D. K. Hartline, P. H. Hartline, and K.-I. Naka for additional support and guidance.

This study is based in large part on a thesis submitted by Dr. Krausz for the Ph.D. degree at the University of California, San Diego, June 1976.

This research was supported primarily by grants from the Sloan Foundation and the United States Public Health Service (N. I. H. grants NS 05628 to W. O. Friesen and NS 05665 to H. I. Krausz).

Received for publication 2 December 1976.

REFERENCES

BLACKMAN, R. B., and J. W. TUKEY. 1959. The Measurement of Power Spectra from the Point of View of Communications Engineering. Dover Publications Inc., New York.

BRILLINGER, D. R. 1975. The identification of point-process systems. *Ann. Prob.* **3**:909–929.

BRYANT, H., and J. P. SEGUNDO. 1976. Spike initiation by transmembrane current; a white-noise analysis. *J. Physiol. (Lond.).* **260**:279–314.

BULLOCK, T. H. 1943. Neuromuscular facilitation in *Scyphomedusae*. *J. Cell. Comp. Physiol.* **22**:251–272.

CAREW, T. J., and E. R. KANDEL. 1974. Synaptic analysis of the interrelationships between behavioral modifications in *Aplysia*. Synaptic Transmission and Neuronal Interaction. Raven Press, Inc., New York. 339–383.

CASTELLUCCI, V., H. PINSKER, I. KUPFERMANN, and E. R. KANDEL. 1970. Neuronal mechanisms of habituation and dishabituation of the gill withdrawal reflex in *Aplysia*. *Science (Wash. D. C.).* **167**:1745–1748.

DEL CASTILLO, J., and B. KATZ. 1954. Statistical factors involved in neuromuscular facilitation and depression. *J. Physiol. (Lond.).* **124**:574–585.

DODGE, F. A., and R. RAHAMIMOFF. 1967. Cooperative action of calcium ions in transmitter release at the neuromuscular junction. *J. Physiol. (Lond.).* **193**:419–432.

DUDEL, J., and S. W. KUFFLER. 1961. Mechanism of facilitation at the crayfish neuromuscular junction. *J. Physiol. (Lond.).* **155**:530–542.

FRIESEN, W. O. 1975. Antifacilitation and facilitation in the cardiac ganglion of the spiny lobster *Panulirus interruptus*. *J. Comp. Physiol.* **101**:207–224.

GERSTEIN, G. L., and N. Y. S. KIANG. 1960. An approach to the quantitative analysis of electrophysiological data from single neurons. *Biophys. J.* **1**:15–28.

HAGIWARA, S. and T. H. BULLOCK. 1957. Intracellular potentials in pacemaker and integrative neurons of the lobster cardiac ganglion. *J. Cell. Comp. Physiol.* **50**:25–47.

HARTLINE, D. K. 1967. Impulse identification and axon mapping of the nine neurons in the cardiac ganglion of the lobster *Homarus americanus*. *J. Exp. Biol.* **47**:327–340.

KRAUSZ, H. I. 1975. Identification of nonlinear systems using random impulse train inputs. *Biol. Cybern.* **19**:217–230.

KRAUSZ, H. I. 1976. Nonlinear analysis of synaptic transmission using random stimulation of a presynaptic axon. Ph.D. Thesis. University of California at San Diego, La Jolla, Calif.

KRAUSZ, H. I., and W. O. FRIESEN. 1975. Identification of discrete input nonlinear systems using Poisson impulse trains. *In* Proceedings First Symposium on Testing and Identification of Nonlinear Systems. G. D. McCann and P. Z. Marmarelis, editors. California Institute of Technology, Pasadena, Calif. 125–146.

LEE, Y. W., and M. SCHETZEN. 1965. Measurement of the Wiener kernels of a nonlinear system by cross-correlation. *Int. J. Control.* **2**:237–254.

LIPSON, E. D. 1975. White noise analysis of *Phycomyces* light growth response system. I. Normal intensity range. *Biophys. J.* **15**:989–1011.

MAGLEBY, K. L. 1973*a*. The effect of repetitive stimulation on transmitter release at the frog neuromuscular junction. *J. Physiol. (Lond.).* **234**:327–352.

MAGLEBY, K. L. 1973*b*. The effect of tetanic and post-tetanic potentiation on facilitation of transmitter release at the frog neuromuscular junction. *J. Physiol. (Lond.).* **234**:353–371.

MAGLEBY, K. L., and J. E. ZENGLE. 1975*a*. A dual effect of repetitive stimulation on tetanic and post-tetanic potentiation of transmitter release at the frog neuromuscular junction. *J. Physiol. (Lond.).* **245**:163–182.

MAGLEBY, K. L., and J. E. ZENGLE. 1975*b*. A quantitative description of tetanic and post-tetanic potentiation of transmitter release at the frog neuromuscular junction. *J. Physiol. (Lond.)*. **245**:183–208.

MALLART, A., and A. R. MARTIN. 1967. An analysis of facilitation of transmitter release at the neuromuscular junction of frog. *J. Physiol. (Lond.)*. **193**:677–694.

MARMARELIS, P. Z. 1975. The noise about white-noise: pros and cons. *In* Proceedings of the First Symposium on Testing and Identification of Nonlinear Systems. G. D. McCann and P. Z. Marmarelis, editors. California Institute of Technology, Pasadena, Calif. 56–75.

MARMARELIS, P. Z., and K.-I. NAKA. 1973*a*. Nonlinear analysis and synthesis of receptive field responses in the catfish retina. I. Horizontal cell chain. *J. Neurophysiol.* **36**:605–618.

MARMARELIS, P. Z., and K.-I. NAKA. 1973*b*. Nonlinear analysis and synthesis of receptive field responses in the catfish retina. II. One-input white-noise analysis. *J. Neurophysiol.* **36**:619–633.

MARMARELIS, P. Z., and K.-I. NAKA. 1973*c*. Nonlinear analysis and synthesis of receptive field responses in the catfish retina. II. Two-input white-noise analysis. *J. Neurophysiol.* **36**:634–648.

MARMARELIS, P. Z., and K.-I. NAKA. 1974. Experimental analysis of a neural system: two modeling approaches. *Kybernetik*. **15**:11–26.

MCCANN, G. D. 1974. Nonlinear identification theory models for successive stages of visual nervous systems in flies. *J. Neurophysiol.* **37**:869–895.

MOORE, G. P., D. G. STUART, E. K. STAUFFER, and R. REINKING. 1975. White-noise analysis of mammalian muscle receptors. *In* Proceedings of the First Symposium on Testing and Identification of Nonlinear Systems. G. D. McCann and P. Z. Marmarelis, editors. California Institute of Technology, Pasadena, Calif. 316–324.

PALM, G., and T. POGGIO. 1977. The Volterra representation and the Wiener expansion: validity and pitfalls. SIAM J. on Appl. Math. In press.

STARK, L. 1968. Neurological Control Systems in Studies in Bioengineering. Plenum Publishing Corp., New York.

TAKEUCHI, A., and N. TAKEUCHI. 1962. Electrical changes in pre and postsynaptic axons of the giant synapse of *Loligo*. *J. Gen. Physiol.* **45**:1181–1193.

WIENER, N. 1958. Nonlinear Problems in Random Theory. John Wiley & Sons, Inc., New York.

VOLTERRA, V. 1959. Theory of Functionals and of Integral and Integro-differential Equations. Dover Publications, New York.

YOUNKIN, S. G. 1974. An analysis of the role of calcium in facilitation at the frog neuromuscular junction. *J. Physiol. (Lond.)*. **237**:1–14.